

Solution Properties of Polymacromonomers Consisting of Polystyrene. 2. Chain Dimensions and Stiffness in Cyclohexane and Toluene

Ken Terao, Yo Nakamura,* and Takashi Norisuye

Department of Macromolecular Science, Osaka University, Machikaneyama-cho 1-1, Toyonaka, Osaka 560-0043, Japan

Received October 22, 1998; Revised Manuscript Received December 15, 1998

ABSTRACT: A series of polymacromonomer samples (F15) consisting only of polystyrene and having a fixed side chain length of 15 styrene residues have been prepared and studied by static light scattering in cyclohexane at different temperatures and in toluene at 15 °C. The measurement has also been made on polymacromonomer samples (F33) of the same kind but with 33 side chain residues in toluene. The second virial coefficient for the F15 polymer in cyclohexane vanishes at 34.5 °C, the Θ temperature for linear polystyrene, as was previously found to be the case for the F33 polymer. Analysis of the measured mean-square radii of gyration based on the wormlike chain with or without excluded volume shows that, while the contour length per main-chain residue is insensitive to the side chain length, the Kuhn segment length λ^{-1} (or more generally the stiffness parameter in the helical wormlike chain) under the Θ condition remarkably increases with increasing side chain length and that the λ^{-1} values (16 and 36 nm) for the polymacromonomers F15 and F33 in toluene, a good solvent, are about 1.6 times as large as those in the Θ solvent. Thus, it is concluded that, in addition to the high segment density around the main chain, repulsions between the main chain and side chain and between neighboring side chains play an important role in the high stiffness of polymacromonomers.

Introduction

As was shown by previous workers,^{1–3} polymacromonomers consisting of the poly(methyl methacrylate) (PMMA) backbone and polystyrene (PS) side chains behave as semiflexible chains in toluene, a good solvent. The origin of this semiflexibility ought to be understood in terms of the molecular architecture and monomer–monomer interactions, but it is yet unclear. Undoubtedly, those polymacromonomers composed of chains of the two different kinds are disadvantageous to use for the study of such interactions. Thus, we recently commenced a series of dilute-solution studies on polymacromonomers consisting only of PS, whose chemical structure is shown in Figure 1.

In the previous paper⁴ (referred to as part 1 of this series), we found from light scattering measurements that a polymacromonomer with a fixed side chain length of 33 styrene residues (designated below as F33) in cyclohexane attains the Θ condition at 34.5 °C, the Θ temperature for linear PS in the same solvent. Analysis of the measured z -average mean-square radii of gyration $\langle S^2 \rangle_z$ based on the wormlike chain⁵ showed its Kuhn segment length λ^{-1} (or more generally the stiffness parameter in the helical wormlike chain⁶) to be 1 order of magnitude larger than that for the linear chain at the Θ point, indicating that the high segment density around the main chain remarkably stiffens the polymacromonomer backbone. As the temperature T increased, both λ^{-1} and excluded-volume strength gradually increased. This finding suggests that the backbone is further stiffened by enhancement of repulsion between the main chain and side chain and between neighboring side chains.

The present study was undertaken to ascertain this suggestion, by extending the light scattering experiment to toluene solutions of the polymacromonomer F33 and also to toluene and cyclohexane solutions of another polymacromonomer F15, i.e., a series of samples with

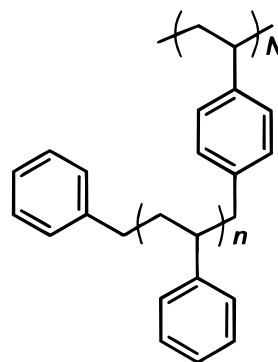


Figure 1. Chemical structure of a polymacromonomer consisting of polystyrene. The main chain and each side chain have degrees of polymerization of N and n , respectively. The polymacromonomer F15 stands for $n = 15$ and the polymacromonomer F33, $n = 33$.

15 styrene side chain residues. The measurement in toluene was made at 15 °C since the unperturbed dimensions and hence the chain stiffness of linear PS at that temperature essentially agreed with those in cyclohexane at 34.5 °C.⁷ Results of $\langle S^2 \rangle_z$ and their analysis based on the wormlike chain are described below, along with the preparation of F15 samples.

Experimental Section

Samples of F15. α -Benzyl- ω -vinylbenzylpolystyrene, the styrene macromonomer, was synthesized by living anionic polymerization in the manner reported by Tsukahara et al.^{8,9} The product was reprecipitated five times from acetone solutions into methanol to remove unreacted p -chloromethylstyrene. Its molecular weight was 1.65×10^3 when estimated from the weight-average molecular weight M_w of 1.53×10^3 determined for the precursor (α -benzyl- ω -hydrogen polystyrene) by light scattering. The weight-average to number-average molecular weight ratio M_w/M_n for the precursor was estimated to be 1.09 by a MALDI-TOF spectrometer with a *trans,trans*-1,4-diphenyl-1,3-butadiene matrix containing silver ions in the

form of AgCF_3COO ; the value of M_w evaluated from the mass spectrum agreed with the light scattering value of 1.53×10^3 within 4%.

The macromonomer was polymerized in benzene at 45–60 °C for 50–100 h with azobis(isobutyronitrile) as an initiator to obtain 12 polymacromonomer samples. The products were purified and extensively fractionated by the procedures employed for F33 samples in part 1.⁴ From the fractions thus obtained, 10 middle ones designated below as F15-1, F15-2, ..., F15-10 were chosen for the present study.

Anionic polymerization was also carried out with the *n*-BuLi/tetramethylethylenediamine/toluene ligand complex as an initiator (at room temperature for 24 h) to prepare five low molecular weight samples. These samples were fractionated by repeated fractional solution with toluene as the solvent and methanol as the precipitant, and appropriate middle fractions designated as F15-11, F15-12, F15-13, F15-14, and F15-15 were added to the above-mentioned 10 samples. Values of M_w/M_n for fractions F15-2, F15-3, ..., F15-13 were estimated by gel permeation chromatography (GPC).

Samples of F33. Two samples designated F33-13 and F33-14 were added to the previously prepared fractions,⁴ F33-1, F33-2, ..., F33-10. They were newly prepared by living anionic polymerization, followed by repeated fractional solution, in the manner described above for low molecular weight samples of F15.

Light Scattering. Scattering intensities were measured for all polymacromonomer samples in toluene at 15 °C and eight samples, F15-1, F15-2, ..., F15-6, F15-8, and F15-12, in cyclohexane at different temperatures on a Fica-50 light scattering photometer in an angular range from 15° to 150°. Vertically polarized incident light of 436 and 546 nm wavelengths was used. The experimental procedures including optical clarification were essentially the same as those described in part 1.⁴ The scattering intensity data obtained were analyzed by use of the square-root plots of $(Kc/R_\theta)^{1/2}$ vs c and $(Kc/R_\theta)^{1/2}$ vs $\sin^2(\theta/2)$, but for the concentration dependence of intensity for cyclohexane solutions, the linear plot of Kc/R_θ vs c was used. Here, K is the optical constant, c the polymer mass concentration, and R_θ the excess reduced scattering intensity at scattering angle θ . The second virial coefficients A_2 of cyclohexane solutions were determined from the data at 546 nm, since, as remarked elsewhere,¹⁰ the attenuation of light by scattering, absorption, and multiple scattering were not always negligible at 436 nm, giving rise to small errors (less than $10^{-5} \text{ mol cm}^3 \text{ g}^{-2}$) in A_2 near the Θ point. Optical anisotropy effects on M_w , $\langle S^2 \rangle_z$, and A_2 were negligible in the range of molecular weight studied.

The specific refractive index increments $\partial n/\partial c$ of the polymacromonomers F33 and F15 in toluene at 15 °C and those of F15 in cyclohexane at 25, 30, 35, and 40 °C were determined for samples F15-5, F15-10, F15-13, and F33-13 using a modified Schulz–Cantow type differential refractometer. The $\partial n/\partial c$ values for toluene solutions were $0.110 \text{ cm}^3 \text{ g}^{-1}$ at 436 nm and $0.106 \text{ cm}^3 \text{ g}^{-1}$ at 546 nm for the F15 polymer and $0.109 \text{ cm}^3 \text{ g}^{-1}$ at 436 nm and $0.105 \text{ cm}^3 \text{ g}^{-1}$ at 546 nm for the F33 polymer at c lower than $2 \times 10^{-2} \text{ g cm}^{-3}$. The results for F15 in cyclohexane were found to be represented by

$$\partial n/\partial c = 3.6 \times 10^{-4} T(^{\circ}\text{C}) + 0.173 \quad (\text{cm}^3 \text{ g}^{-1}; \lambda_0 = 436 \text{ nm})$$

$$\partial n/\partial c = 3.6 \times 10^{-4} T(^{\circ}\text{C}) + 0.159 \quad (\text{cm}^3 \text{ g}^{-1}; \lambda_0 = 546 \text{ nm})$$

at $c \leq 1.5 \times 10^{-2} \text{ g cm}^{-3}$.

Results

Second Virial Coefficient. Figure 2 illustrates the concentration dependence of Kc/R_θ for sample F15-4 in cyclohexane at the indicated temperatures, where R_θ denotes the zero-angle value of R_θ . The straight lines fitting the plotted points at the respective T converge to a common intercept, yielding an identical M_w within experimental error. The values of A_2 evaluated from

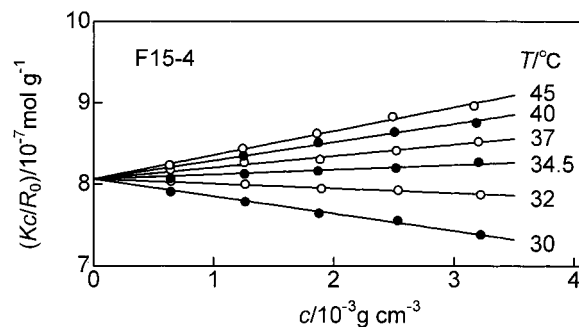


Figure 2. Concentration dependence of Kc/R_θ for polymacromonomer sample F15-4 in cyclohexane at indicated temperatures. Wavelength = 546 nm.

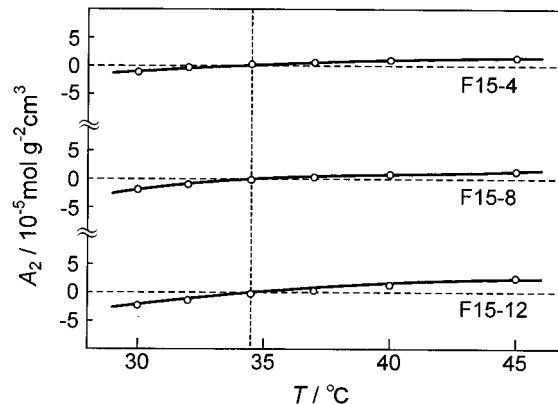


Figure 3. Temperature dependence of A_2 for polymacromonomer samples F15-4, F15-8, and F15-12 in cyclohexane. The vertical dashed line indicates 34.5 °C (the Θ temperature).

their slopes are plotted against T in Figure 3, along with those for samples F15-8 and F15-12 in the same solvent. The second virial coefficients for the three samples vanish at 34.5 °C, showing that the polymacromonomer F15 in cyclohexane attains the Θ condition at this temperature, as is the case with linear PS and the polymacromonomer F33.⁴ This strongly suggests that, for polymacromonomers of the kind shown in Figure 1, the Θ temperature is essentially independent of side chain length, at least, for n (the degree of polymerization of each side chain) ≤ 33 .

Interestingly, however, the T dependence of A_2 in Figure 3 is much weaker than that known for linear PS¹¹ and slightly stronger than what we previously found for the F33 polymer,⁴ so that an effect of side chain length appears in the magnitude of (dA_2/dT) at the Θ point. We note that because of the T -insensitive behavior of A_2 , the Θ temperature of 34.5 °C for the polymacromonomer F15 + cyclohexane system is accurate to ± 1 °C.

Figure 4 illustrates the molecular weight dependence of A_2 for F15 and F33 in toluene at 15 °C. The curves for both polymers have a very large negative slope of -0.80 at low M_w and a small (or usual) negative slope of about -0.20 at high M_w . For $M_w > 6 \times 10^5$, the values of A_2 are all on the order $10^{-5} \text{ mol cm}^3 \text{ g}^{-2}$, but those for the F33 polymer are systematically smaller.

Radius of Gyration. The temperature dependence of $\langle S^2 \rangle_z$ for six samples of the polymacromonomer F15 in cyclohexane is illustrated in Figure 5. It is much weaker than that¹² for linear PS with the same molecular weight in cyclohexane but not as weak as what we previously found for the F33 polymer in the same solvent.⁴

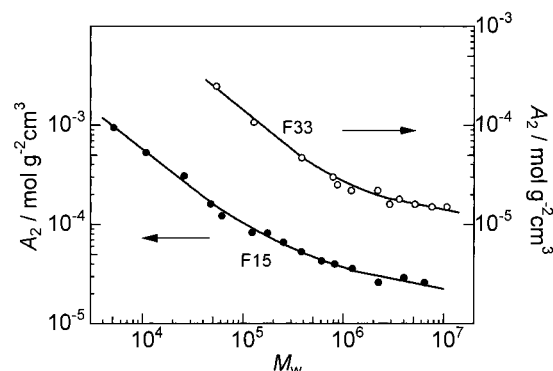


Figure 4. Molecular weight dependence of A_2 for the polymacromonomers F15 (filled circles) and F33 (unfilled circles) in toluene at 15 °C.

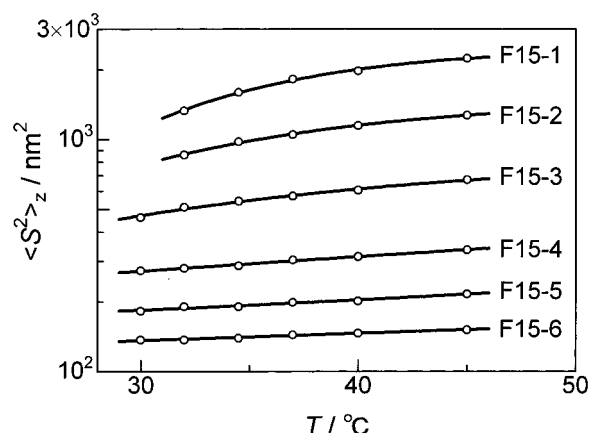


Figure 5. Temperature dependence of $\langle S^2 \rangle_z$ for the indicated F15 samples in cyclohexane.

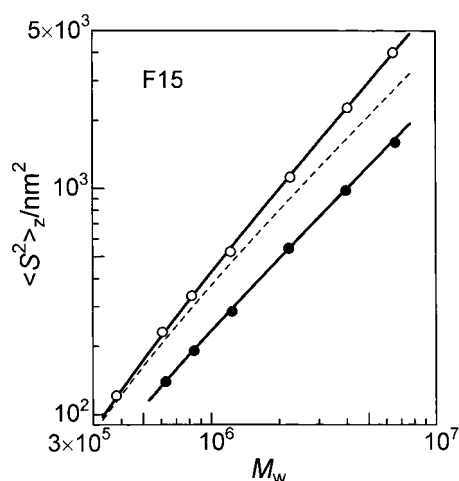


Figure 6. Molecular weight dependence of $\langle S^2 \rangle_z$ for the polymacromonomer F15 in cyclohexane at 34.5 °C (filled circles) and in toluene at 15 °C (unfilled circles). Solid curves, theoretical values calculated from eqs 1 and 3 with the parameters in Table 4; dashed lines, theoretical values for $B = 0$.

Figure 6 shows the molecular weight dependence of $\langle S^2 \rangle_z$ for the polymacromonomer F15 in cyclohexane at Θ (34.5 °C) and in toluene at 15 °C. The indicated solid and dashed lines are explained in the Discussion section. We here note that the curve for cyclohexane solutions has a slope 1.1 for $M_w < 1 \times 10^6$ and 1.0 for $M_w > 2 \times 10^6$, while the solid curve for toluene solutions has a slope 1.4 for $M_w < 8 \times 10^5$ and 1.2 for $M_w > 2 \times$

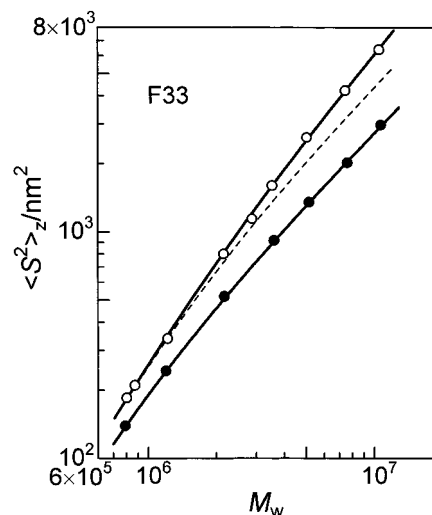


Figure 7. Molecular weight dependence of $\langle S^2 \rangle_z$ for the polymacromonomer F33 in toluene at 15 °C (unfilled circles) and in cyclohexane at 34.5 °C (filled circles; reproductions from ref 4). Solid curves represent theoretical values calculated from eqs 1 and 3 with the parameters in Table 4; dashed lines represent theoretical values for $B = 0$.

Table 1. Results from Light Scattering Measurements on Polymacromonomer F15 Samples in Cyclohexane at Different Temperatures

sample	$M_w/10^5$	$\langle S^2 \rangle_z/10^2 \text{ nm}^2$					
		30 °C	32 °C	34.5 °C	37 °C	40 °C	45 °C
F15-1	66.1		13.3	16.0	18.2	19.8	22.5
F15-2	39.8		8.58	9.80	10.5	11.5	12.7
F15-3	22.1	4.62	5.11	5.43	5.71	6.05	6.71
F15-4	12.4	2.72	2.79	2.86	3.03	3.13	3.35
F15-5	8.41	1.82	1.90	1.90	1.99	2.02	2.16
F15-6	6.29	1.37	1.37	1.39	1.44	1.46	1.51
F15-8	2.54						
F15-12	0.470						

Table 2. Results from Light Scattering Measurements on Polymacromonomer F15 Samples in Toluene at 15 °C

sample	$M_w/10^5$	$10^5 A_2/\text{cm}^3 \text{ mol g}^{-2}$	$\langle S^2 \rangle_z/10^2 \text{ nm}^2$	M_w/M_n^a
F15-1	64.7	2.6	40.1	
F15-2	40.4	2.9	22.8	1.08
F15-3	22.5	2.6	11.2	1.07
F15-4	12.3	3.6	5.24	1.06
F15-5	8.22	4.0	3.35	1.05
F15-6	6.09	4.3	2.31	1.06
F15-7	3.81	5.3	1.21	1.08
F15-8	2.52	6.6		1.09
F15-9	1.75	8.2		1.10
F15-10	1.23	8.3		1.10
F15-11	0.614	12.2		1.08
F15-12	0.474	16.1		1.09
F15-13	0.260	30.8		1.09
F15-14	0.108	53.0		
F15-15	0.0514	94.6		

^a From GPC with chloroform as the eluent.

10^6 . Similar plots of $\log \langle S^2 \rangle_z$ vs $\log M_w$ for the polymacromonomer F33 in the two solvents are displayed in Figure 7, in which the cyclohexane data are the reproductions from our previous work.⁴ The slope of the solid curve for toluene solutions decreases from 1.6 to 1.2 with increasing M_w .

Numerical results from light scattering and GPC measurements are summarized in Tables 1–3; only the M_w value for 546 nm at 34.5 °C is given for each sample in Table 1, since it agreed with those obtained for the

Table 3. Results from Light Scattering Measurements on Polymacromonomer F33 Samples in Toluene at 15 °C

sample	$M_w/10^5$	$10^5 A_2/\text{cm}^3 \text{ mol g}^{-2}$	$\langle S^2 \rangle_z/10^2 \text{ nm}^2$	M_w/M_n^b
F33-1	108 (106 ^a)	1.5	64.0	
F33-2	76.5 (75.0 ^a)	1.5	42.1	1.10 ^c
F33-3	51.7 (50.5 ^a)	1.6	26.1	1.08 ^c
F33-4	36.2 (35.5 ^a)	1.8	16.0	1.06 ^c
F33-5	28.9	1.6	11.4	1.06
F33-6	22.0 (21.8 ^a)	2.2	8.01	1.06 ^c
F33-7	12.0 (12.2 ^a)	2.2	3.39	1.04 ^c
F33-8	8.73	2.5	2.10	1.10
F33-9	7.90 (8.03 ^a)	3.0	1.85	1.05 ^c
F33-10	3.84	4.7		1.12
F33-13	1.28	10.7		
F33-14	0.543	24.7		

^a In cyclohexane (ref 4). ^b From GPC with chloroform as the eluent. ^c Reference 4.

two wavelengths at different temperatures within $\pm 1\%$. A few remarks may be made here. First, the M_w values determined in toluene and cyclohexane agree with each other within $\pm 1.7\%$. Second, the samples examined by GPC are narrow in molecular weight distribution. The z -average to weight-average molecular weight ratios M_z/M_w (not shown here) were essentially the same as the M_w/M_n values for the respective samples.

Discussion

Data Analysis. 1. *Polymacromonomer F15 in Cyclohexane.* We model the polymacromonomer F15 of high molecular weight by the wormlike chain, whose unperturbed mean-square radius of gyration, $\langle S^2 \rangle_0$, is given by¹³

$$\lambda^2 \langle S^2 \rangle_0 = \frac{\lambda L}{6} - \frac{1}{4} + \frac{1}{4\lambda L} - \frac{1}{8(\lambda L)^2} [1 - \exp(-2\lambda L)] \quad (1)$$

Here, L is the contour length of the main chain related to the molecular weight M by $L = M/M_L$, with M_L being the molar mass per unit contour length. Unless the main chain of the polymacromonomer is sufficiently long compared to each side chain, the replacement of the polymer with the infinitely thin wormlike chain ceases to be valid. In part 1 of this series, we examined the validity of this replacement, i.e., the effects of chain thickness and chain ends on $\langle S^2 \rangle$, by evaluating the radius of gyration of a wormlike polymacromonomer whose side chains are flexible (but yet wormlike) and linked to the stiffer backbone by completely flexible joints. Note that the end effect may be significant if side chains near the main-chain ends contribute toward apparently increasing L . The calculation showed the side chain effects to be insignificant for the F33 polymacromonomer with $\langle S^2 \rangle_0 \geq 140 \text{ nm}^2$ or $M \geq 8 \times 10^5$. For the F15 polymer, we found that the corresponding condition is given by $\langle S^2 \rangle_0 \geq 70 \text{ nm}^2$. Since our F15 samples all satisfy this condition, we may conclude that the present analysis requires no consideration of the side chain effects.

Equation 1 can be approximated by¹⁴

$$\left(\frac{M}{\langle S^2 \rangle_0} \right)^{1/2} = (6\lambda M_L)^{1/2} \left(1 + \frac{3M_L}{4\lambda M} \right) \quad (2)$$

with the maximum error from the exact value being 1% for $\lambda L > 2$. Panel a of Figure 8 shows the plot of $(M_w/\langle S^2 \rangle_z)^{1/2}$ vs M_w^{-1} constructed from our $\langle S^2 \rangle_z$ data in

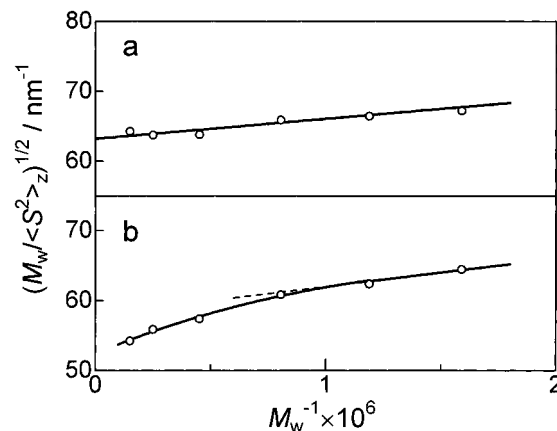


Figure 8. Plots of $(M_w/\langle S^2 \rangle_z)^{1/2}$ vs M_w^{-1} for the polymacromonomer F15 in cyclohexane at the Θ temperature (a) and at 45 °C (b).

cyclohexane at the Θ temperature according to eq 2. The data points follow a straight line, whose intercept and slope yield $9.5 \pm 0.5 \text{ nm}$ for λ^{-1} and $6200 \pm 200 \text{ nm}^{-1}$ for M_L . The curve closely fitting the filled circles in Figure 6 represents the theoretical values calculated from eq 1 with $\lambda^{-1} = 9.5 \text{ nm}$ and $M_L = 6200 \text{ nm}^{-1}$. The corresponding solid line drawn for the cyclohexane data in Figure 7 represents eq 1 with $\lambda^{-1} = 22 \text{ nm}$ and $M_L = 13\,000 \text{ nm}^{-1}$.⁴

Panel b of Figure 8 shows that the $\langle S^2 \rangle_z$ data in cyclohexane at 45 °C do not obey the linear relation of $(M_w/\langle S^2 \rangle_z)^{1/2}$ vs M_w^{-1} . This can be ascribed to excluded-volume effects. We analyze $\langle S^2 \rangle_z$ data in cyclohexane at temperatures other than Θ with the aid of the quasi-two-parameter (QTP) theory^{6,15,16} for wormlike or helical wormlike bead chains. This theory allows an accurate description of $\langle S^2 \rangle$ for linear flexible and semiflexible polymers^{7,17–20} over a broad range of molecular weight.

The radius expansion factor $\alpha_s \equiv (\langle S^2 \rangle / \langle S^2 \rangle_0)^{1/2}$ in the QTP scheme is expressed by

$$\alpha_s^2 = \left[1 + 10\tilde{z} + \left(\frac{70\pi}{9} + \frac{10}{3} \right) \tilde{z}^2 + 8\pi^{3/2} \tilde{z}^3 \right]^{2/15} [0.933 + 0.067 \exp(-0.85\tilde{z} - 1.39\tilde{z}^2)] \quad (3)$$

if the Domb–Barrett function²¹ is adopted. Here, \tilde{z} is the scaled excluded-volume parameter defined by

$$\tilde{z} = \frac{3}{4} K(\lambda L) z \quad (4)$$

with

$$z = \left(\frac{3}{2\pi} \right)^{3/2} (\lambda B)(\lambda L)^{1/2} \quad (5)$$

and

$$\begin{aligned} K(\lambda L) &= \frac{4}{3} - 2.711(\lambda L)^{-1/2} + \frac{7}{6}(\lambda L)^{-1} \quad \text{for } \lambda L > 6 \\ &= (\lambda L)^{-1/2} \exp[-6.611(\lambda L)^{-1} + 0.9198 + 0.03516\lambda L] \quad \text{for } \lambda L \leq 6 \end{aligned} \quad (6)$$

In eq 5, z is the conventional excluded-volume parameter and B is the excluded-volume strength defined for the wormlike chain by

$$B = \beta/a^2 \quad (7)$$

Table 4. Wormlike Chain Parameters and Excluded-Volume Strength for the Polymacromonomers F15 and F33 in Cyclohexane at Different Temperatures and in Toluene at 15 °C

polymer	solvent	$T/^\circ\text{C}$	λ^{-1}/nm	$M_L/10^3\text{nm}^{-1}$	B/nm
F15	cyclohexane	32	9.4	6.2 ^a	-0.4
F15	cyclohexane	34.5	9.5	6.2	0
F15	cyclohexane	37	9.5	6.2 ^a	0.3
F15	cyclohexane	40	9.6	6.2 ^a	0.6
F15	cyclohexane	45	9.8	6.2 ^a	1.2
F15	toluene	15	16	6.2 ^a	4.5
F33	cyclohexane	32	21 ^b	13.0 ^b	-0.4 ^b
F33	cyclohexane	34.5	22 ^b	13.0 ^b	0 ^b
F33	cyclohexane	37	23 ^b	13.0 ^b	0.5 ^b
F33	cyclohexane	40	23 ^b	13.0 ^b	1.5 ^b
F33	cyclohexane	45	24 ^b	13.0 ^b	2.4 ^b
F33	toluene	15	36	13.0 ^a	18

^a Assumed. ^b Reference 4.

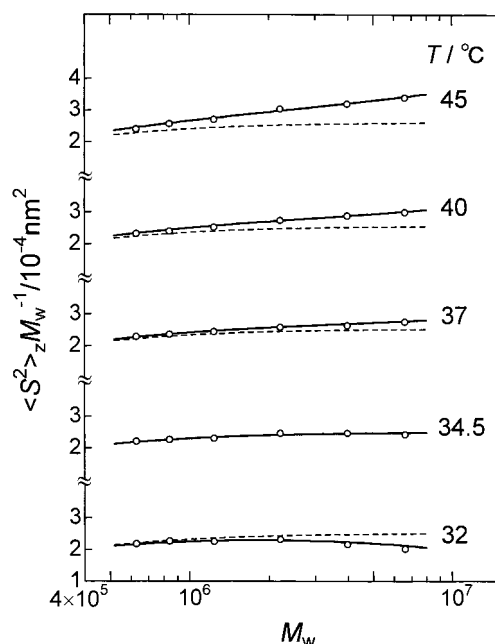


Figure 9. Comparison between the measured $\langle S^2 \rangle_z$ vs M_w^{-1} for the polymacromonomer F15 in cyclohexane at indicated temperatures and the theoretical values (solid lines) calculated from eqs 1 and 3 with the parameters in Table 4. Dashed lines represent theoretical values for $B = 0$.

with β and a being the binary cluster integral representing the interaction between a pair of beads and the bead spacing, respectively. In our case, one bead must contain a number of main-chain residues but need not be specified.

Equations 3–7 indicate that B needs to be known (in addition to λ^{-1} and M_L) in order to evaluate theoretical α_s^2 and hence theoretical $\langle S^2 \rangle$ in a perturbed state. A curve-fitting procedure was employed for the determination of the parameters, but M_L at any T was assumed to be the same as that in cyclohexane at 34.5 °C; we note that the three parameters could not uniquely be determined from the $\langle S^2 \rangle_z$ data because of the strong correlation between λ^{-1} and B in the molecular weight range studied here. The parameters obtained are summarized in Table 4, in which our previous estimates for the polymacromonomer F33 in cyclohexane are also presented for comparison. Figure 9 compares the experimental $\langle S^2 \rangle_z M_w^{-1}$ for the F15 polymer in cyclohexane with the theoretical solid lines calculated from eqs 1 and 3 with the parameters in Table 4. The agreement is

satisfactory at any temperatures. The dashed line at each T refers to the unperturbed state (i.e., $B = 0$). Excluded-volume effects are appreciable at any temperatures other than Θ . In particular, at 45 °C they appear over the entire range of M_w studied.

2. Polymacromonomers F15 and F33 in Toluene. The $\langle S^2 \rangle_z$ data for the two polymers in toluene do not follow the linear relation (eq 2) between $(M_w/\langle S^2 \rangle_z)^{1/2}$ and M_w^{-1} for unperturbed wormlike chains. Thus, their analysis was made in the way used above for cyclohexane solutions near Θ , assuming that M_L for each polymer in toluene is the same as that in cyclohexane at 34.5 °C. The parameters thus obtained are included in Table 4.

The solid lines drawn for the toluene data in Figures 6 and 7 represent the theoretical $\langle S^2 \rangle$ values calculated from eqs 1 and 3 with the parameters in Table 4. They closely fit the unfilled circles for the respective polymacromonomers. The dashed line in either figure again refers to the unperturbed state. Its pronounced downward deviation from the corresponding solid curve substantiates that consideration of excluded-volume effects is important to the experimental estimation of λ^{-1} , at least, for our polymacromonomers in toluene, a good solvent.

Effects of Side Chain Length and Solvent on Molecular Characteristics. We discuss the model parameters summarized in Table 4. The M_L value of 6200 nm⁻¹ for the polymacromonomer F15 (in cyclohexane at the Θ temperature) with the molar mass (1650) of the macromonomer yields 0.27 nm for the contour length per main-chain residue. This length is essentially identical to that (0.27 nm) for the F33 polymer,⁴ suggesting that the local conformation of the PS backbone is insensitive to the side chain length. The monomeric contour length of 0.27 nm does not differ from the value of 0.25 nm calculated on the assumption that the backbone assumes the all-trans conformation. The slightly larger experimental estimate becomes very close to the all-trans value if M_L is corrected for the polydispersity ($M_d/M_w = 1.06$) of our samples (F15-2 through F15-6) in the analysis of $\langle S^2 \rangle_z$ by replacing L in eq 1 with the z -average $L (= M_d/M_L)$; note that for $M > 6 \times 10^5$ $\langle S^2 \rangle_0$ is determined substantially by the first two leading terms of eq 1.

While the contour length per main-chain residue is insensitive to the side chain length, λ^{-1} is an increasing function of it. The λ^{-1} value of 9.5 nm for the F15 polymer in cyclohexane at 34.5 °C is less than one-half that for F33 in the same solvent but much larger than that (2 nm) for the linear PS molecule modeled by the wormlike chain;²² note that linear PS is better modeled by the helical wormlike chain and that λ^{-1} (the stiffness parameter) in this model is 2.1–2.7 nm.^{23–26} The pronounced effect of side chain length on λ^{-1} , observed here, is in line with what was found by Wintermantel et al.² for polymacromonomers consisting of the PMMA backbone and PS side chains in toluene.

As the temperature increases, λ^{-1} and B for the F15 polymer in cyclohexane gradually increase, being also in line with our previous finding for F33 in the same solvent (see Table 4). For both polymers, the parameters in toluene are much larger than those in cyclohexane near Θ , the increases of λ^{-1} amounting to 1.6 times. This ascertains our previous suggestion (mentioned in the Introduction) that enhancement of side chain–side chain or main chain–side chain repulsion stiffens the

polymacromonomer backbone. Another finding (in Table 4) that B in toluene is larger for F33 than for F15 seems reasonable because one bead for the former polymer must contain a larger number of monomeric units.

Conclusions

We have determined $\langle S^2 \rangle_z$ and A_2 as functions of total weight-average molecular weight for two polymacromonomers consisting of polystyrene with fixed side chain residues of 15 (F15) and 33 (F33) in cyclohexane at different temperatures (only for F15) and in toluene at 15 °C. The polymacromonomer F15 has been found to attain the Θ state in the former solvent at 34.5 °C, as is the case with the polymacromonomer F33 and linear polystyrene. The following conclusions have been drawn from the analysis of $\langle S^2 \rangle_z$ data based on the wormlike chain with or without excluded volume.

1. The contour length per main-chain residue is quite insensitive to the side chain length.

2. In cyclohexane at the Θ point, the Kuhn segment length λ^{-1} (or more generally the stiffness parameter in the helical wormlike chain) remarkably increases (from about 2 nm for linear PS to 22 nm for F33) with increasing side chain length. Thus, even in the absence of intramolecular excluded-volume interaction (in the conventional framework), the semiflexibility of polymacromonomers arises from the high segment density around the main chain.

3. As the excluded-volume strength increases in cyclohexane, λ^{-1} gradually increases, and in toluene, a good solvent for the two polymacromonomers F15 and F33, it becomes almost 1.6 times as large as that in the Θ state. Hence, main chain–side chain and side chain–side chain repulsions are also responsible for the semiflexibility of polymacromonomers.

Acknowledgment. We are very grateful to Professor Jimmy W. Mays of the University of Alabama at Birmingham for his help in MALDI-TOF mass spectroscopy.

References and Notes

- (1) Wintermantel, M.; Schmidt, M.; Tsukahara, Y.; Kajiwara, K.; Kohjiya, S. *Macromol. Rapid Commun.* **1994**, *15*, 279.
- (2) Wintermantel, M.; Gerle, M.; Fischer, K.; Schmidt, M.; Wataoka, I.; Urakawa, H.; Kajiwara, K.; Tsukahara, Y. *Macromolecules* **1996**, *29*, 978.
- (3) Nemoto, N.; Nagai, M.; Koike, A.; Okada, S. *Macromolecules* **1995**, *28*, 3854.
- (4) Terao, K.; Takeo, Y.; Tazaki, M.; Nakamura, Y.; Norisuye, T. *Polym. J.* **1999**, *31*, 193.
- (5) Kratky O.; Porod, G. *Recl. Trav. Chim. Pays-Bas* **1949**, *68*, 1106.
- (6) Yamakawa, H. *Helical Wormlike Chains in Polymer Solutions*; Springer: Berlin, 1997.
- (7) Abe, F.; Einaga, Y.; Yoshizaki, T.; Yamakawa, H. *Macromolecules* **1993**, *26*, 1884.
- (8) Tsukahara, Y. In *Macromolecular Design: Concept and Practice*; Mishra, M. K., Ed.; Polymer Frontiers International: New York, 1994; pp 161–227.
- (9) Tsukahara, Y.; Inoue, J.; Ohta, Y.; Kohjiya, S.; Okamoto, Y. *Polym. J.* **1994**, *26*, 1013.
- (10) Okumoto, M.; Terao, K.; Nakamura, Y.; Norisuye, T.; Teramoto, A. *Macromolecules* **1997**, *30*, 7493.
- (11) See, for example: Nakamura, Y.; Norisuye, T.; Teramoto, A. *Macromolecules* **1991**, *24*, 4904.
- (12) See, for example: Miyaki, Y. Ph.D. Thesis, Osaka University, 1981.
- (13) Benoit, H.; Doty, P. *J. Phys. Chem.* **1953**, *57*, 958.
- (14) Murakami, H.; Norisuye, T.; Fujita, H. *Macromolecules* **1980**, *13*, 345.
- (15) Yamakawa, H.; Stockmayer, W. H. *J. Chem. Phys.* **1972**, *57*, 2843.
- (16) Shimada, J.; Yamakawa, H. *J. Chem. Phys.* **1986**, *85*, 591.
- (17) Horita, K.; Abe, F.; Einaga, Y.; Yamakawa, H. *Macromolecules* **1993**, *26*, 5067.
- (18) Abe, F.; Horita, K.; Einaga, Y.; Yamakawa, H. *Macromolecules* **1994**, *27*, 725.
- (19) Kamijo, M.; Abe, F.; Einaga, Y.; Yamakawa, H. *Macromolecules* **1995**, *28*, 1095.
- (20) Norisuye, T.; Tsuboi, A.; Teramoto, A. *Polym. J.* **1996**, *28*, 357.
- (21) Domb, C.; Barrett, A. J. *Polymer* **1976**, *17*, 179.
- (22) Norisuye, T.; Fujita, H. *Polym. J.* **1982**, *14*, 143.
- (23) Einaga, Y.; Koyana, H.; Konishi, T.; Yamakawa, H. *Macromolecules* **1989**, *22*, 3419.
- (24) Konishi, T.; Yoshizaki, T.; Saito, T.; Einaga, Y.; Yamakawa, H. *Macromolecules* **1990**, *23*, 290.
- (25) Konishi, T.; Yoshizaki, T.; Yamakawa, H. *Macromolecules* **1991**, *24*, 5614.
- (26) Yamada, T.; Yoshizaki, T.; Yamakawa, H. *Macromolecules* **1992**, *25*, 377.

MA9816517